ELSEVIER

Journal of Chromatography A, 772 (1997) 115–127

JOURNAL OF CHROMATOGRAPHY A

Electroinjection analysis
Concept, mathematical model and applications

Victor P. Andreev*, Natalia B. Ilyina, Elena V. Lebedeva, Alexandr G. Kamenev, Nicolai S. Popov

Institute for Analytical Instrumentation, Russian Academy of Sciences, 26 pr. Rigsky, St. Petersburg, 198103, Russia

Abstract

Electroinjection analysis is described and compared with electrophoretically mediated microanalysis and flow injection analysis. Mathematical models of electroinjection analysis and electrophoretically mediated microanalysis are presented. An analytical solution for the concentration of the product of a chemical reaction is derived and used for the discussion of the optimal regimes of analysis. Examples of the applications of electroinjection analysis and electrophoretically mediated microanalysis for the determination of Cr(VI) and Co(II) ions in water are presented.

Keywords: Electroinjection analysis; Mathematical models; Electrophoretically mediated microanalysis; Metal cations

1. Introduction

A new combination of flow injection analysis (FIA) and capillary zone electrophoresis (CZE) has been proposed recently [1,2] and called electroinjection analysis (EIA).

According to this method, sample and reagent are simultaneously injected from the opposite ends of the capillary, electrokinetically. They meet in the capillary, go through one another and react. The product of the reaction can be detected, for example, photometrically. Due to the presence of electroosmotic flow, it is possible to mix in this way not only oppositely charged sample and reagent but even reactants with the same charge, when their electrophoretic mobilities are different. Due to the absence of flow non-uniformity, there is no Taylor dispersion, the additional dispersion due to sample and reagent mixing is also absent, so the peak broadening in EIA is much smaller than in FIA and that is why the sensitivity is higher. EIA has much in common with electrophoretically mediated microanalysis (EMMA) [3–5]. In both methods (EMMA and EIA), mixing of sample and reagent takes place in the capillary with a longitudinal electric field applied and is due to the difference in electrophoretic mobilities of the reactants. However, in EMMA, sample and reagent are injected from the same end of the capillary while in EIA they are injected from opposite ends of the capillary. Electrophoretic movement of sample and reagents in opposite directions was also realized in Refs. [6,7]. However, in both papers, sample and reagent were initially injected hydrostatically from the same end of the capillary, and only then was the electric field applied and they started moving electrophoretically in opposite directions. The stage of the hydrostatic injection adds to the universality of the method but definitely enlarges band broadening and reduces sensitivity, due to the non-uniformity of the flow profile during the hydrostatic injection.

As shown in Ref. [2], both EIA and EMMA have some limitations, as far as the values and signs of

*Corresponding author.

PII S0021-9673(97)00112-X

electrophoretic mobilities of the reactants are concerned. However, any pair of reactants can be mixed either by EIA or EMMA, except in the case where both reactants have zero charge. These methods are not conflicting at all. They can be combined or realized with the same instrument, a capillary electrophoresis system with two samplers, designed to be capable of injecting reactants from both ends of the capillary simultaneously. EMMA is better for the case where reactants have electrophoretic mobilities of the same sign as the electroosmotic mobility of the buffer electrolyte. For EIA, there is only one important limitation: The reactant that is injected in the direction opposite to the direction of electroosmotic flow must have electrophoretic mobility of the opposite sign and it must be higher than the electroosmotic mobility of the buffer. However, in the case where electrophoretic mobilities of the reactants have values that permit the use of either method, it seems that EIA has some advantages over EMMA. First is the possibility of using very short capillaries for EIA and, consequently, being able to use lower electric fields. In EMMA, there is the critical mixing length needed to mix reactants, which is determined by the difference in the electrophoretic mobilities of the reactants [2]; if this difference is small, the critical mixing length can be quite significant. Secondly, in EMMA, cross-contamination of sample and reagent is possible at the introduction end of the capillary, while during EIA, it is impossible because sample and reagent are injected through opposite ends of the capillary. Thirdly, in the case of sorption of the reactants on the capillary wall during EMMA, there might be chemical interaction between moving and sorbed ions, which might lead to the tailing of the product peak, while in EIA, sample and reagent move in different paths and such interaction is impossible.

EIA and EMMA have common advantages over FIA. The first is the absence of band broadening due to the Taylor dispersion and mixing. Second is the separation of sample components due to intrinsic electrophoresis and, consequently, the reduction of matrix effects. Third is that the typical injection volumes of sample and reagent in EIA and EMMA are about 0.05 μl, which is at least two orders of magnitude smaller than during FIA, and so, very low amounts of sample and reagent are consumed.

In this paper, the mathematical model of EIA and EMMA is presented. Analytical solutions for the concentration of the chemical reaction product are produced and used for the discussion of the optimal regime for EIA and EMMA. Determination of Cr(VI) according to EIA and determination of Co(II) according to EMMA are presented in the experimental section of the paper.

2. Mathematical model of EIA and EMMA

In Ref. [2], we presented a simplistic model of sample and reagent mixing in EIA. That model was suitable only for fast chemical reactions and equal concentrations of both reactants. In Ref. [5], the mathematical model of EMMA, based on numerical simulation, was presented. In this paper, we present a new mathematical model of EIA and EMMA. This model is more realistic than the model of Ref. [2] and, unlike Ref. [5], it provides the possibility of obtaining analytical solutions that would be useful for optimization.

Consider a sample and reagent that are forced to move by a longitudinal electric field, E, with different velocities along a cylindrical tube of infinite length and radius, a. The situation is depicted in Fig. 1.

We make the following assumptions:

(1) The concentrations of sample, reagent and product are much smaller than the concentration of buffer electrolyte, so that local conductivity and local electric field are independent of the presence of sample, reagent and product and are considered to be constant.

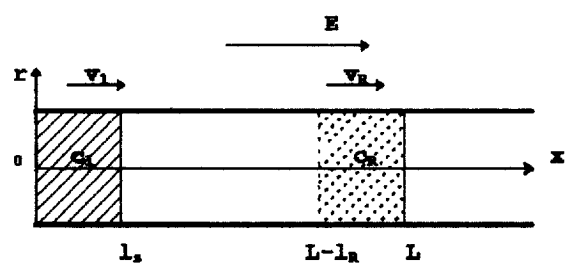

Fig. 1. Illustration of the initial distribution of sample and reagent in the capillary tube for the mathematical model of EMMA and EIA: for EMMA $v_R>0$; for EIA $v_R<0$.

(2) There is no sorption of sample, reagent and product on the walls of the tube and no particle-wall interactions.

(3) Velocities of sample, reagent and product (v_1, v_R, v_2) are considered to be independent of longitudinal and radial coordinates. This assumption is valid if:

(a) The zeta-potential of the wall is constant along the tube;

(b) the buffer concentration is equal to, or higher than, 1×10^{-3} M, then electroosmotic velocity dependence on the radial coordinate can be ignored [8];

(c) the influence of temperature effects on buffer viscosity and reactants' electrophoretic mobility can be ignored (the validity of this assumption is also discussed in [8]).

With these assumptions, the problem is reduced to one-dimension and the evolution of sample, reagent and product concentrations c_1, c_R, c_2 can be described by the following set of equations:

$$\frac{\partial c_1}{\partial t} + v_1 \frac{\partial c_1}{\partial x} = D_1 \frac{\partial^2 c_1}{\partial x^2} - k_- c_1 c_R + k_- c_2$$

$$\frac{\partial c_R}{\partial t} + v_R \frac{\partial c_R}{\partial x} = D_R \frac{\partial^2 c_R}{\partial x^2} - k_+ c_1 c_R + k_- c_2$$

$$\frac{\partial c_2}{\partial t} + v_2 \frac{\partial c_2}{\partial x} = D_2 \frac{\partial^2 c_2}{\partial x^2} + k_- c_1 c_R - k_- c_2 \qquad (1)$$

with initial conditions

$$c_1 = \begin{cases} c_{10}, & 0 < x < l_S \\ 0, & x < 0, x > l_S \end{cases}, t = 0 \qquad (2)$$

$$c_R = \begin{cases} c_{R0}, & L - l_R < x < L \\ 0, & x < L - l_R, x > L' \end{cases}, t = 0 \qquad (3)$$

$$c_2 = 0, t = 0 \qquad (4)$$

where D_1, D_R, D_2 are sample, reagent and product diffusion coefficients, and k_+, k_- are direct and reverse reaction rates, respectively.

Initial conditions, Eqs. (2)–(4) mean that sample and reagent are initially localized in some parts of the tube that are spatially separated and that the product is initially absent. The set of equations in Eq. (1) describe both EIA and EMMA. In the case of EMMA, the sign of v_R is the same as the sign of v_1, while in the case of EIA, v_R is negative.

Up to this stage, the assumptions of the model and the set of equations (given in Eq. (1)) are equivalent to the model studied in [5] with the only difference being that in Ref. [5], a single-substrate enzymatic reaction was studied and, therefore, the kinetic terms of the equations were different. In Ref. [5], the model was studied with the help of numerical simulations and it is quite natural because the set of equations (Eq. (1)) cannot be solved analytically. To get the analytical solution, let us use the second group of assumptions that are valid for most of the practical cases of EIA and EMMA:

(1) The initial concentration of the reagent, c_{R0}, is much higher than the initial concentration of the sample, c_{10}, and so, the concentration of reagent in the moving reagent zone can be considered to be constant.

(2) The time of analysis is much smaller than the diffusion time. The time of analysis in EIA is

$$t_a = L/(|v_R| + |v_1|)$$

and in EMMA, it is

$$t_a = L/|v_R - v_1|$$

Diffusion time is

$$t_D = \min\left\{\frac{l_S^2}{D_1}, \frac{l_R^2}{D_R}\right\}.$$

For typical values: $L = 10$ cm, $l_S = 1$ cm, $l_R = 1$ cm, $v_1 = 0.1$ cm/s, $v_R = 0.05$ cm/s, $D = 1\cdot10^{-5}$ cm^2/s, we have

$$t_{a,EIA} = 60 \text{ s}, t_{a,EMMA} = 200 \text{ s}, t_D = 1\cdot10^5 \text{ s}$$

so that this assumption is good enough and enables us to ignore the diffusion terms in Eq. (1).

(3) The reverse reaction is considered to be much slower than the forward reaction, and so, reverse reaction terms are ignored.

This second group of assumptions leads us to the simplified set of equations:

$$\frac{\partial c_1}{\partial t} + v_1 \frac{\partial c_1}{\partial x} = -k(x - v_R t)\cdot c_1 \qquad (5)$$

$$\frac{\partial c_2}{\partial t} + v_2 \frac{\partial c_2}{\partial x} = k(x - v_R t)\cdot c_1 \qquad (6)$$

$$k(z)=\begin{cases}k_0 & L-l_R<z<L\\ 0 & z<L-l_R, z>L\end{cases} \quad (7)$$

where

$k_0 = k_+ c_{R0}$

with initial conditions

$$t=0 \quad c_1=\begin{cases}c_{10}, & 0<x<l_S\\ 0, & x<0, x>l_S\end{cases} \quad (8)$$

$$t=0 \quad c_2=0 \quad (9)$$

Here, the fact that reagent is localized in the zone moving with the velocity, v_R, is taken into consideration by the functional dependence (Eq. (7)) of the effective reaction rate constant, k, on $x-v_Rt$.

An analytical solution to Eqs. (5) and (6) with the conditions given in Eqs. (7)–(9) was produced with the help of the following change of variables:

$$\begin{cases}x\rightarrow\eta=x-v_1t\\ t\rightarrow T=t\end{cases}$$

So that Eq. (5) was transformed to:

$$\frac{\partial c_1}{\partial T}=-k(\eta+(v_1-v_R)T)\cdot c_1(\eta,T) \quad (10)$$

with initial conditions of

$$c_1(\eta,0)=\begin{cases}c_{10}, & 0<\eta<l_S\\ 0, & \eta<0, \eta>l_S\end{cases} \quad (11)$$

where

$$k(\eta+(v_1-v_R)T)=\begin{cases}k_0, & \dfrac{L-l_R-\eta}{v_1-v_R}\le T\le\dfrac{L-\eta}{v_1-v_R}\\ 0, & T<\dfrac{L-l_R-\eta}{v_1-v_R}, T>\dfrac{L-\eta}{v_1-v_R}\end{cases} \quad (12)$$

Naturally, condition $v_1>v_R$ is always valid, otherwise the reactants would never meet.

The solution to Eq. (10) is quite evident:

$$c_1(\eta,T)=c_1(\eta,0)\exp\left(-\int_0^T k(\eta+(v_1-v_R)T)\,dT\right) \quad (13)$$

where $c_1(\eta, 0)$ is determined by Eq. (11) and $k(\eta+(v_1-v_R)T)$ by Eq. (12).

The solution to Eq. (13) can be rewritten as:

$$c_1(\eta,T)=\begin{Bmatrix}c_{10}, & 0\le\eta\le l_S\\ 0, & \eta<0, \eta>l_S\end{Bmatrix} \cdot \begin{cases}1, T<\dfrac{L-l_R-\eta}{v_1-v_R}\\ \exp\left(-k_0\left(T-\dfrac{L-l_R-\eta}{v_1-v_R}\right)\right), \dfrac{L-l_R-\eta}{v_1-v_R}\le T\le\dfrac{L-\eta}{v_1-v_R}\\ \exp\left(-k_0\dfrac{l_R}{v_1-v_R}\right), T>\dfrac{L-\eta}{v_1-v_R}\end{cases} \quad (14)$$

To solve Eq. (6), let us again change the variables:

$$\begin{cases}x\rightarrow\xi=x-v_2t=\eta+(v_1-v_2)t\\ t\rightarrow\tau=t=T\end{cases}$$

so that Eq. (6) will have the form:

$$\frac{\partial c_2}{\partial\tau}=k(\xi+(v_2-v_R)\tau)\cdot c_1(\xi,\tau) \quad (15)$$

where, by substituting new variables into Eqs. (14) and (17), we get:

$$c_1(\xi,\tau)=\begin{Bmatrix}c_{10}, & -\xi<(v_2-v_1)\tau<l_S-\xi\\ 0, & (v_2-v_1)\tau<-\xi, (v_2-v_1)\tau>l_S-\xi\end{Bmatrix} \cdot \begin{cases}1, \tau(v_2-v_R)<L-l_R-\xi\\ \exp\left(-k_0\dfrac{\tau(v_2-v_R)-L+l_R+\xi}{v_1-v_R}\right), L-l_R-\xi\le\tau(v_2-v_R)\le L-\xi\\ \exp\left(-k_0\dfrac{l_R}{v_1-v_R}\right), \tau(v_2-v_R)>L-\xi\end{cases} \quad (16)$$

$$k(\xi+(v_2-v_R)\tau)=\begin{cases}k_0, & L-l_R-\xi\le(v_2-v_R)\tau\le L-\xi\\ 0, & (v_2-v_R)\tau<L-l_R-\xi\\ 0, & (v_2-v_R)\tau>L-\xi\end{cases} \quad (17)$$

The solution of Eq. (15) is naturally

$$c_2=\int_0^\tau k(\xi+(v_2-v_R)\tau)\cdot c_1(\xi,\tau)\,d\tau \quad (18)$$

however, to get it in explicit form, one must know if the differences in velocities (v_2-v_R) and (v_2-v_1) are positive or negative and what the relationships are between L, l_R and l_S. Cases where the velocity differences are equal to zero must be treated separately as special cases. Details of the solution are presented in Appendix A.

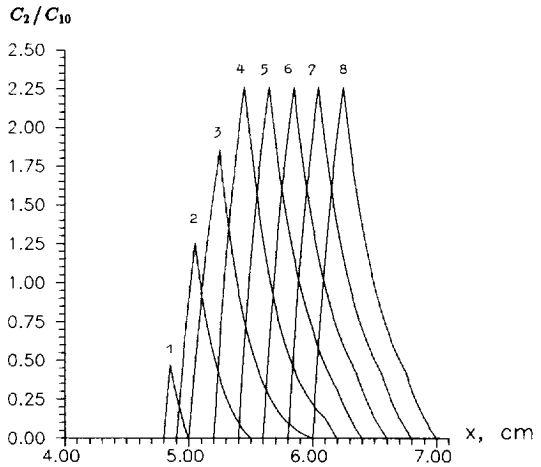

Fig. 2. Mathematical modelling of EMMA. Product concentration versus coordinate for different values of time: $k_0=1\ s^{-1}$, $v_1=0.5$ cm/s, $v_R=0.1$ cm/s, $v_2=0.2$ cm/s, $L=5$ cm, $l_S=1$ cm, $l_R=1$ cm, 1, 2, 3, 4, 5, 6, 7 and 8-$t=8$, 9, 10, 11, 12, 13, 14 and 15 s, respectively.

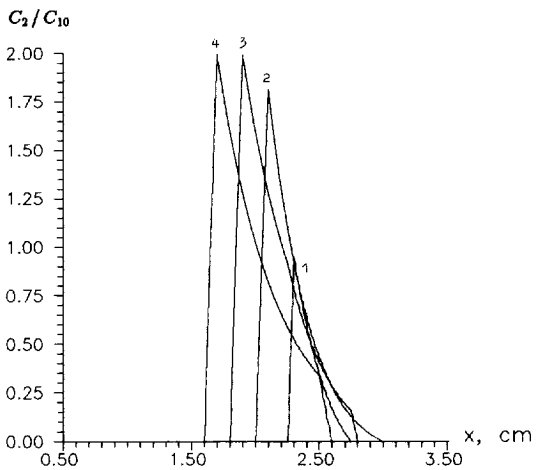

Fig. 4. Mathematical modeling of EIA. Product concentration versus coordinate for different values of time. Product and reagent are moving in the same direction: $k_0=1\ s^{-1}$, $v_1=0.25$ cm/s, $v_R=-0.25$ cm/s, $v_2=-0.2$ cm/s, $L=5$ cm, $l_S=1$ cm, $l_R=1$ cm, 1, 2, 3 and 4-$t=7$, 8, 9 and 10 s, respectively.

3. Results of the model and discussion

Figs. 2–8 present the dependences of product concentration on coordinate for different moments of time. To calculate these dependences, we substituted $\xi = x - v_2 t$ into Eqs. (A4–A9, A15, A18).

Figs. 2–5 correspond to the case of a rather slow chemical reaction, $k_0=1\ s^{-1}$. The characteristic time of the chemical reaction here is commensurable with the time of interaction of the sample and reagent zones. Fig. 2 corresponds to the case of EMMA while Figs. 3–5 correspond to EIA. Fig. 3 presents the case when the product is moving in the opposite direction to that of the reagent, while Fig. 4 presents

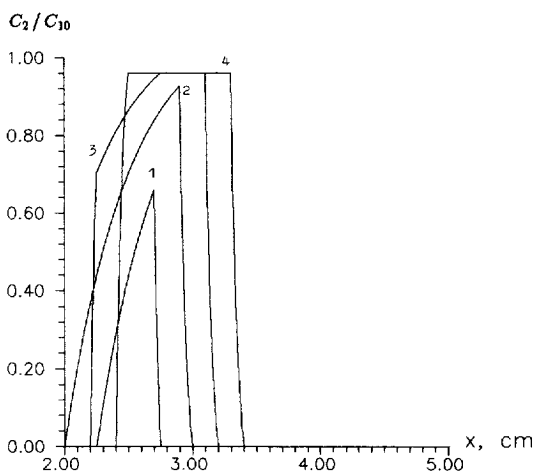

Fig. 3. Mathematical modeling of EIA. Product concentration versus coordinate for different values of time. Product and reagent are moving in opposite directions: $k_0=1\ s^{-1}$, $v_1=0.25$ cm/s, $v_R=-0.25$ cm/s, $v_2=0.2$ cm/s, $L=5$ cm, $l_S=1$ cm, $l_R=1$ cm, 1, 2, 3 and 4-$t=7$, 8, 9 and 10 s, respectively.

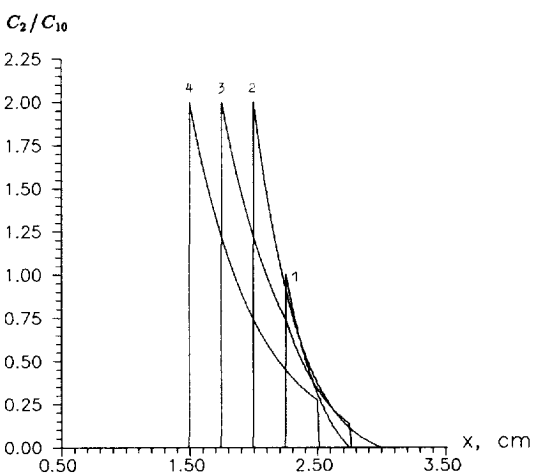

Fig. 5. Mathematical modeling of EIA. Product concentration versus coordinate for different values of time. Product and reagent are moving with the same velocity: $k_0=1\ s^{-1}$, $v_1=0.25$ cm/s, $v_R=v_2=-0.25$ cm/s, $L=5$ cm, $l_S=1$ cm, $l_R=1$ cm, 1, 2, 3, 4-$t=7$ s, 8 s, 9 s, 10 s.

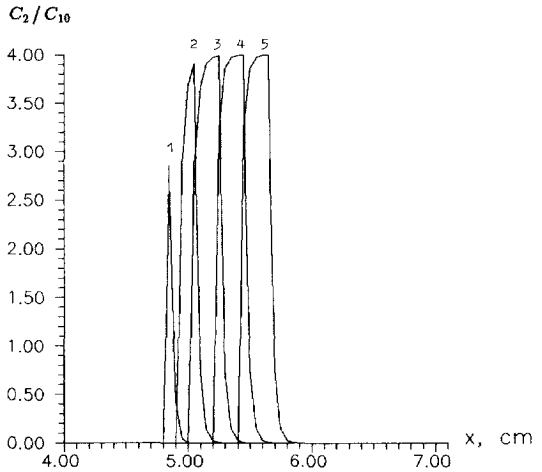

Fig. 6. Mathematical modeling of EMMA. Product concentration versus coordinate for different values of time: $k_0 = 10\ s^{-1}$, $v_1 = 0.5$ cm/s, $v_R = 0.1$ cm/s, $v_2 = 0.2$ cm/s, $L = 5$ cm, $l_S = 1$ cm, $l_R = 1$ cm, 1, 2, 3, 4 and 5-t = 8, 9, 10, 11 and 12 s, respectively.

the case when the product is moving in the same direction as the reagent. Fig. 5 corresponds to the special case when the velocity of the product is equal to the velocity of the reagent. Figs. 6–8 correspond to the same cases as Figs. 2–4, but for the faster chemical reactions, $k_0 = 10\ s^{-1}$, so the slopes of the product peaks in Figs. 6–8 are much steeper.

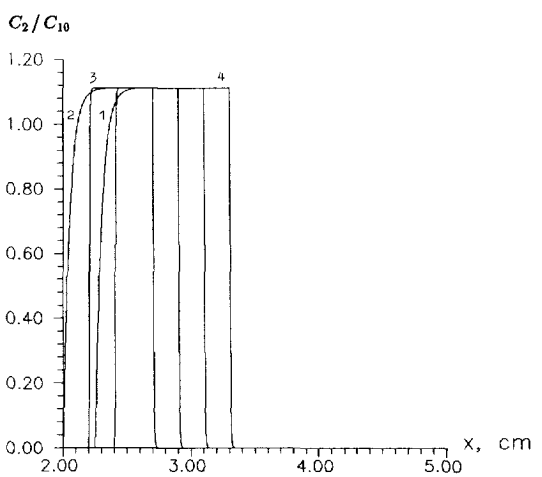

Fig. 7. Mathematical modeling of EIA. Product concentration versus coordinate for different values of time. Product and reagent are moving in the opposite directions: $k_0 = 10\ s^{-1}$, $v_1 = 0.25$ cm/s, $v_R = -0.25$ cm/s, $v_2 = 0.2$ cm/s, $L = 5$ cm, $l_S = 1$ cm, $l_R = 1$ cm, 1, 2, 3 and 4-t = 7, 8, 9 and 10 s, respectively.

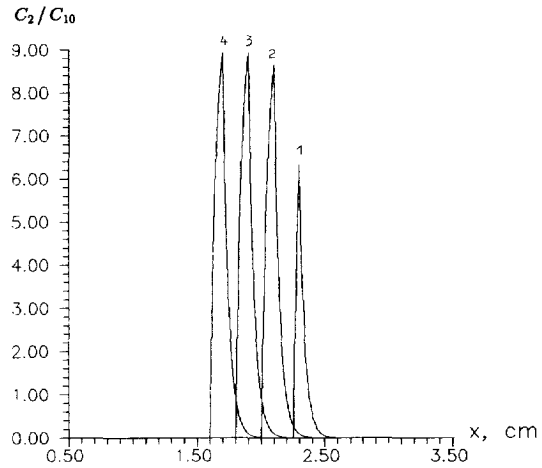

Fig. 8. Mathematical modeling of EIA. Product concentration versus coordinate for different values of time. Product and reagent are moving in the same direction: $k_0 = 10\ s^{-1}$, $v_1 = 0.25$ cm/s, $v_R = -0.25$ cm/s, $v_2 = -0.2$ cm/s, $L = 5$ cm, $l_S = 1$ cm, $l_R = 1$ cm, 1, 2, 3 and 4-t = 7, 8, 9 and 10 s, respectively.

The important feature that is characteristic for all figures is that the amplitude of the peaks is increasing with time, till some time value, after which, the amplitude stops increasing. Then the form of the peak remains constant and it is simply moving along the tube with a constant velocity.

The time value when the peak amplitude reaches its maximum corresponds to the moment when sample and reagent zones have passed through one another and are not in contact any more. After that moment, there is no more product formation.

The forms of the peaks are quite different in the cases when the velocity of the product has the same sign as the velocity of the reagent and when the signs of the these velocities are different. When the product is moving in the same direction as the reagent, the portions of the product formed at the different time moments concentrate in the same spatial zone, so the product peak is high and narrow, and one has a kind of kinematical focusing. If the signs of v_2 and v_R are different, then the newly formed portions of product lag behind the previously formed portions of product and the product peak is wide and low. Figs. 2–8 also help us to understand the importance of the right choice of detector positions. For example, if the coordinate of the detector for the case presented in Fig. 2 is $x_D \leq 5$ cm,

then the peak amplitude will be nearly five times smaller than the amplitude of the peak detected by the same detector positioned at the point with coordinate $x_D \geq 5.5$ cm. Similarly, for the case presented in Fig. 4, the peak amplitude for $x_D > 2.2$ cm is two times smaller than the peak amplitude for $x_D < 2.0$ cm. Unfortunate choices of detector position correspond to situations where the product peak is passing the detector at the moment when sample and reagent zones are still interacting and product formation is not complete.

Analysis of the solution determined by Eqs. (A4)–(A9), (A16), (A18), (A20) gives very simple and exact formulae for the maximum values of product concentration that can be achieved during the analysis.

If $v_2 \neq v_R$ then:

$$(1)\quad c_{2max} = c_{10}\frac{v_1 - v_R}{|v_R - v_2|} \times \left[1 - \exp\left(-k_0 \frac{l_R}{v_1 - v_R}\right)\right] \quad \text{if } \frac{l_S}{l_R} > \left|\frac{v_1 - v_2}{v_R - v_2}\right| \tag{19}$$

$$(2)\quad c_{2max} = c_{10}\frac{v_1 - v_R}{|v_R - v_2|} \times \left[1 - \exp\left(-k_0 \frac{l_S|v_R - v_2|}{|v_1 - v_2|(v_1 - v_R)}\right)\right] \quad \text{if } \frac{l_S}{l_R} < \left|\frac{v_1 - v_2}{v_R - v_2}\right| \tag{20}$$

For $v_2 = v_R$:

$$c_{2max} = c_{10}k_0 \frac{l_S}{v_1 - v_2} \tag{21}$$

It can be easily seen that Eq. (21) can be produced not only by treating the special case shown in Eq. (A18), but also formally as a limiting form of Eq. (20), when $v_R \to v_2$.

Eq. (19) also works if $v_2 = v_1$, then the condition

$$\frac{l_S}{l_R} > \left|\frac{v_1 - v_2}{v_R - v_2}\right|$$

always holds and

$$c_{2max} = c_{10}\left[1 - \exp\left(-k_0 \frac{l_R}{v_1 - v_R}\right)\right] \tag{22}$$

.

The same result can be produced by the treatment of the special case (see Eq. (A19)).

By analyzing Eqs. (19), (20), (22), one can see that the maximum values of the product concentration are determined by two factors: f_1 and f_2. The first factor is $f_1 = 1 - \exp(-k_0 t_{int})$, where t_{int} is the time of sample zone and reagent zone interaction:

$$t_{int} = \frac{l_R}{v_1 - v_R}, \text{ if } \frac{l_S}{l_R} > \left|\frac{v_1 - v_2}{v_R - v_2}\right|,$$

and

$$t_{int} = \frac{l_S|v_R - v_2|}{|v_1 - v_2|(v_1 - v_R)}, \text{ if } \frac{l_S}{l_R} < \left|\frac{v_1 - v_2}{v_R - v_2}\right|$$

This factor characterizes the amount of sample that has been transformed into product during the interaction of the zones.

The second factor, f_2:

$$f_2 = \left|\frac{v_1 - v_2}{v_R - v_2}\right|$$

is the kinematical focusing factor that determines how the product that is formed is distributed in the time and space domain.

For the fast chemical reaction, $k_0 t_{int} \gg 1$, and $f_1 \approx 1$, practically all of the sample is transformed into the product. It means that the amount of product formed is practically equal to the initial amount of sample, $c_{10}l_S$. The amplitude of the product peak and its width is then determined by the factor f_2. If f_2 is large, then the peak is high and narrow, and if f_2 is small, then the peak is low and wide. The width of the peak can be characterized by:

$$\delta = c_{10}l_S/c_{2max} \approx \frac{l_S|v_R - v_2|}{v_1 - v_R}, v_2 \neq v_R \tag{23}$$

$$\delta = c_{10}l_S/c_{2max} = \frac{v_1 - v_2}{k_0}, v_2 = v_R \tag{24}$$

So, the peak is higher and narrower the smaller the difference is between velocities of the product and the reagent. To get the narrow peak, it is important that the product is moving in the same direction as the reagent. Then the sign of v_2 is the same as the

sign of v_R, $|v_R - v_2|$ is small and f_2 is large, so that there is a kinematical focusing.

From Eqs. (21) and (24), it can be seen that the highest and narrowest product peak is formed in the case $v_1 = v_2 = v_R$, then c_{2max} goes to infinity and the peak width, δ, goes to zero. This case corresponds to EMMA but the condition $v_R = v_1$ means that the sample needs infinite time to pass through the reagent and so the time of analysis will, in this case, also be infinite.

The special case of $v_2 = v_R$ is evidently the best as far as kinematical focusing is concerned. To satisfy this condition, the product and reagent must have the same electrophoretic mobility, for example, it can occur when both product and reagent are neutral and are moving with the electroosmotic velocity of the flow.

For EMMA, v_R is positive, while for EIA, v_R is negative; factor f_2 is larger if v_R and v_2 are negative, which means that for fast chemical reactions when $k_0 t_{int} \gg 1$, c_{2max} for EIA can be much larger than for EMMA and this increase of sensitivity due to kinematical focusing does not lead to an increase in the analysis time. Further optimization of the EIA and EMMA regimes must be connected with the choice of experimental conditions that will lead (for the given sample and reagent) to an increase in the factor f_2 that is equal to

$$f_2 = \left|\frac{\mu_{1ep} - \mu_{Rep}}{\mu_{Rep} - \mu_{2ep}}\right|,$$

where μ_{1ep}, μ_{Rep} and μ_{2ep} are the electrophoretic mobilities of sample, reagent and product, respectively.

4. Experimental

4.1. Equipment

Experiments were performed with a laboratory-made capillary electrophoresis system that has been described previously [2]. Detection was photometrical at $\lambda_{max} = 500$ nm for the Co–4-(2-pyrydylazo)resorcinol, disodium salt (PAR) complex and at $\lambda_{max} = 540$ nm for the determination of Cr(VI) with diphenylcarbazide. Fused-silica capillaries (120 μm I.D. × 380 μm O.D.) with a total length of 65 cm for Co and 35 cm for Cr were used. The detector was placed 15 cm from the capillary outlet (cathode). Every day before work, capillaries were conditioned with 0.1 *M* NaOH for 5 min, then rinsed with water and running buffer for no less than 5 min.

4.2. Chemicals

All chemicals used were of analytical grade. Borate buffer (10 m*M*, pH = 9.2) was prepared by dissolving 3.8 g of $Na_2B_4O_7 \cdot 10H_2O$ in 1 l of distilled water. Succinic acid (0.08 *M*), neutralized with NaOH to pH 6.0, was added to the borate to final concentration of 8 m*M* in order to decrease the sorption of metal ions onto the capillary walls. For 2.5 m*M* phosphate buffer, 0.35 g of NaH_2PO_4 was dissolved in 1 l of distilled water, and the pH was adjusted to 2.1 with 0.1 *M* H_2SO_4. Phosphate buffer (5 m*M*), pH 6.9 and a standard phosphate mixture (0.025 *M* KH_2PO_4 and 0.025 *M* K_2HPO_4), pH 6.86 diluted ten-fold were used.

Reagents were prepared as follows: A 0.065-g amount of PAR was dissolved in 25 ml of distilled water to give a 10-m*M* solution and this was diluted with borate–succinate buffer to a concentration of 0.5 m*M* before use. Diphenylcarbazide was dissolved in pure acetone (0.3 g to 30 ml) and stored in the dark. It was diluted ten-fold with phosphate running buffer, pH 2.1, before use, to give an approximately 0.1% (12 m*M*) solution.

Stock solutions of metal salts (1 g of the metal/l) were prepared from $Co(NO_3)_2 \cdot 6H_2O$ and $(NH_4)_2Fe(SO_4)_2 \cdot 7H_2O$ and their concentration was checked by EDTA titration; 0.5 g of $K_2Cr_2O_7$ was dissolved in 100 ml of distilled water to get a 5-mg/ml stock solution.

4.3. Procedure

Electrokinetic injection of sample and reagent was used in both series of experiments.

(a) PAR solution (0.5 m*M*) was injected first for 10 s, +12 kV and then the sample was injected in the same way from the same end of the capillary. HCl (0.1 *M*) was added to the sample to a final concentration of 1 m*M* to stabilize its ionic strength

and prevent hydrolysis. The running voltage was +12 kV with a current of 30–35 μA.

(b) A 0.1% solution of diphenylcarbazide and a standard solution of Cr(VI) (sample) were injected simultaneously from the anode and cathode ends of the capillary. The injection was held at 10 kV for 1 min. The running voltage was 10 kV, the current was 25–30 μA and the analysis time did not exceed 5 min.

Product peak height (in mm) was accepted as the analytical parameter.

4.4. Experimental results and discussion

4.4.1. Determination of cobalt with PAR

PAR is a well-known reagent for the spectrophotometric detection of some metal ions. The reaction with PAR in the CE system using on-column complexation was used previously for the complex determination of some metal ions [9].

For the determination of Co under CE conditions, PAR has the advantages of (1) high sensitivity (ε= 38 000) and (2) during the reaction, Co(II) is oxidized to Co(III), and its complex with PAR can be well separated from complexes of divalent cations. We propose an EMMA method for the quantitation of Co in water that is both rapid and convenient.

Fig. 9 shows electropherograms of standard solutions containing 10, 20 and 40 ng/ml of Co (peak 1). Peak 2 corresponds to PAR itself, and peak 3 corresponds to the Fe(II)-PAR complex produced by admixtures of iron in water or chemicals and by some contamination from the metal parts of the CE system. The amplitudes of peaks 1 and 2 are reproducible, while that of the Fe peak is not, however, it does not affect the determination of Co. The calibration graph for Co in the range of 10–70 ng/ml Co showed good reproducibility and linearity. The linear regression equation, $y=a+bx$ was $h=0.13+1.39C_{Co}$, $s_a=2.1$, $s_b=0.05$ (s is standard deviation), correlation coefficient $r=0.94$ for six data points, each measured three times. The limit of detection ($S/N=3$) was about 1 ng/ml Co.

A sample of tap water containing a large amount of iron (estimated as 0.1 μg/ml using two external Fe(II) standards) was analysed. No significant amount of cobalt (1 ng/ml) was found, so the sample was spiked with 20 and 38 ng/ml Co. The

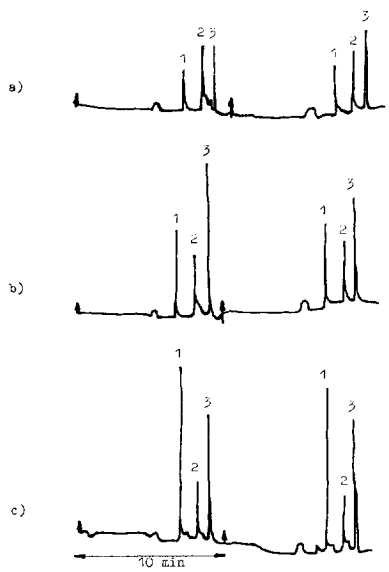

Fig. 9. Electropherograms obtained from three different Co concentrations: (a) 10, (b) 20 and (c) 40 ng/ml. Conditions: 10 m*M* sodium tetraborate, 8 m*M* sodium succinate, pH=9.2; PAR concentration, 0.5 m*M*; sample, 1 m*M*, HCl added; voltage, +12 kV; current, 30 μA; injection, electrokinetic, 12 kV, 10 s. Peak identification: 1=Co–PAR complex, 2=PAR, 3=Fe(II)–PAR complex.

results obtained were 18.4±1.1 and 35±3 ng/ml Co ($n=3$), respectively. So, the effects of the water matrix were hardly observed. The analysis time was about 10 min and could be reduced by using higher fields or shorter capillaries, because Co peak separation was good.

(b) The reaction of Cr(VI) with diphenylcarbazide to form a red complex of Cr(III)-diphenylcarbazone is widely used for the spectrophotometric determination and speciation of chromium. This reaction was easily realized in the EIA regime because the CrO_4^{2-} ion has high negative electrophoretic mobility, and the reagent is practically neutral. However, the reaction proceeds quickly when the acid (usually H_2SO_4) concentration is higher than $1\cdot10^{-2}$ *M*. Acids at these concentrations can hardly be used as running buffers in CE systems because of their extremely high conductivity. Therefore, acid was replaced with 2.5 m*M* phosphate buffer, pH 2.1, but the reaction was rather slow, and we had to use unusually long times for sample and reagent in-

jection to provide sufficient time for the interaction of the zones.

It is desirable that some electrolyte should be introduced into the sample to stabilize its ionic strength. Two variants were tried: (1) dissolving the sample in running buffer and (2) in phosphate buffer, pH 6.9, at a concentration of 5 m*M*. Thus, in this case, electrostacking takes place and the product peak becomes sharper. The two-fold increase in peak amplitude in (2), connected with the lower conductivity of the neutral buffer, was observed. Furthermore, acidification of the real water sample before analysis is not possible because of the fast reduction of Cr(VI) by organic matter of the sample. So, dissolving the sample in neutral buffer was chosen for calibration.

Fig. 10 presents the typical shape of the product peak for chromate concentrations of 50, 100, 150 and 200 ng/ml. By introducing lower concentrations of the buffer into the sample, one can use electrostacking to determine low concentrations of chromate. The calibration graph for 2–14 ng/ml of Cr(VI) was obtained by preparing standard solutions with 1 m*M* phosphate buffer, pH 6.9. The equation of linear regression was $h=-1.2+4.0\ C_{Cr}$, $s_a=1.8$, $s_b=0.2$, correlation coefficient $r=0.989$ (seven points, each measured twice). The limit of detection ($S/N=3$) was 1.4 ng/ml Cr. For 50–250 ng/ml of chromate and with a phosphate concentration of 5 m*M* (pH 6.9), the calibration equation was $h=1.0+0.29\ C_{Cr}$, $s_a=2.9$, $s_b=0.2$, correlation coefficient $r=0.990$ (five points, each measured three times). Therefore, the analytical range can be changed easily by varying the sample buffer concentration.

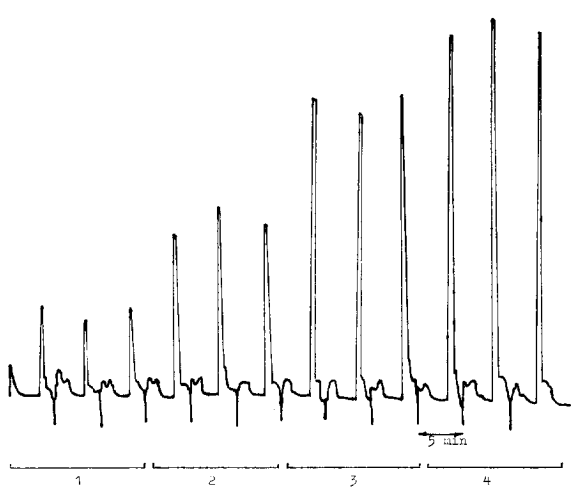

Fig. 10. A series of product peaks in the determination of Cr(IV) with diphenylcarbazide corresponding to (1) 50; (2) 100; (3) 150 and (4) 200 ng/ml Cr. Conditions: 2.5 m*M* sodium phosphate buffer, pH 2.1; reagent concentration, 0.1%; sample, 5 m*M* phosphate buffer, pH 6.9; voltage, 10 kV; current, 35 μA; injection, electrokinetic, 10 kV, 1 min.

5. Conclusion

Electroinjection analysis and electrophoretically mediated microanalysis are a pair of mutually complementary methods that have some advantages over flow injection analysis, such as high quality of mixing, the absence of Taylor dispersion and the separation of sample components due to intrinsic capillary electrophoresis. Mathematical models of EIA and EMMA and the analytical solution derived from them provided an opportunity to understand the influence of differences in electrophoretic mobilities of the sample, reagent and product on the shape and amplitude of the product peak. Kinematical focusing of the product that takes place in the case of optimal ratios of mobilities can enhance the sensitivity of the analysis significantly.

Examples of the usage of EIA and EMMA for the determination of metal ions in water with a 1 ppb detection limit level are presented. Further experimental studies will be focused at the enhancement of analysis sensitivity by exploring the experimental conditions that enlarge the kinematical focusing factor, f_2.

Appendix 1

I. Let us first study the case: $v_R<v_1<v_2$ and define:

$$A=\frac{-\xi}{v_2-v_1},\ B=\frac{l_S-\xi}{v_2-v_1},\ C=\frac{L-l_R-\xi}{v_2-v_R},$$
$$D=\frac{L-\xi}{v_2-v_R} \qquad \text{(A1)}$$

Then, Eq. (16) can be rewritten as:

$$c_1(\xi,\tau)=\left\{\begin{matrix} c_{10}, & A\le\tau\le B \\ 0, & \tau<A,\tau>B \end{matrix}\right\} \cdot \begin{cases} 1, & \tau<C \\ \exp\left(-k_0\dfrac{\pi(v_2-v_R)-L+l_R+\xi}{v_1-v_R}\right), & C\le\tau\le D \\ \exp\left(-k_0\dfrac{l_R}{v_1-v_R}\right), & \tau>D \end{cases} \tag{A2}$$

and Eq. (17) as

$$k(\xi+(v_2-v_R)\tau)=\begin{cases} k_0, & C\le\tau\le D \\ 0, & \tau<C,\tau>D \end{cases} \tag{A3}$$

Evidently $A<B$ and $C<D$, so there are six possible relationships between A, B, C and D:

(1) $A<B\le C<D$

(2) $A\le C\le B\le D$

(3) $A\le C<D\le B$

(4) $C<D\le A<B$

(5) $C\le A\le D\le B$

(6) $C\le A<B\le D$

(1) As can be easily seen if $A<B\le C<D$, then either c_1 or k are equal to zero everywhere and so c_2, defined by Eq. (18), is also equal to zero:

$$c_2=0, A<B\le C<D \tag{A4}$$

(2) If A≤C≤B≤D, then there is only one interval $C<\tau<B$ where both c_1 and k are non-zero and so:

$$c_2=\begin{cases} 0, & \tau<C \\ c_{10}\dfrac{v_1-v_R}{v_R-v_2}\exp\left(k_0\dfrac{L-l_R-\xi}{v_1-v_R}\right)\left(\exp\left(k_0\tau\dfrac{v_R-v_2}{v_1-v_R}\right)-\exp\left(k_0C\dfrac{v_R-v_2}{v_1-v_R}\right)\right), & C\le\tau\le B \\ c_{10}\dfrac{v_1-v_R}{v_R-v_2}\exp\left(k_0\dfrac{L-l_R-\xi}{v_1-v_R}\right)\left(\exp\left(k_0B\dfrac{v_R-v_2}{v_1-v_R}\right)-\exp\left(k_0C\dfrac{v_R-v_2}{v_1-v_R}\right)\right), & \tau>B \end{cases}$$

$$A\le C<B\le D \tag{A5}$$

(3) If $A\le C<D\le B$ then c_1 and k are both non-zero only in the interval $C<\tau<D$ and so:

$$c_2=\begin{cases} 0, & \tau<C \\ c_{10}\dfrac{v_1-v_R}{v_R-v_2}\exp\left(k_0\dfrac{L-l_R-\xi}{v_1-v_R}\right)\left(\exp\left(k_0\tau\dfrac{v_R-v_2}{v_1-v_R}\right)-\exp\left(k_0C\dfrac{v_R-v_2}{v_1-v_R}\right)\right), & C\le\tau\le D \\ c_{10}\dfrac{v_1-v_R}{v_R-v_2}\exp\left(k_0\dfrac{L-l_R-\xi}{v_1-v_R}\right)\left(\exp\left(k_0D\dfrac{v_R-v_2}{v_1-v_R}\right)-\exp\left(k_0C\dfrac{v_R-v_2}{v_1-v_R}\right)\right), & \tau>D \end{cases}$$

$$A\le C<D\le B \tag{A6}$$

(4) If $C<D\le A<B$ then either c_1 or k is equal to zero in every interval and so

$$c_2=0, C<D\le A<B \tag{A7}$$

(5) If $C\le A<D\le B$ then c_1 and k are both non-zero only in the interval $A\le\tau\le D$ and so:

$$c_2=\begin{cases} 0, & \tau<A \\ c_{10}\dfrac{v_1-v_R}{v_R-v_2}\exp\left(k_0\dfrac{L-l_R-\xi}{v_1-v_R}\right)\left(\exp\left(k_0\tau\dfrac{v_R-v_2}{v_1-v_R}\right)-\exp\left(k_0A\dfrac{v_R-v_2}{v_1-v_R}\right)\right), & A\le\tau\le D \\ c_{10}\dfrac{v_1-v_R}{v_R-v_2}\exp\left(k_0\dfrac{L-l_R-\xi}{v_1-v_R}\right)\left(\exp\left(k_0D\dfrac{v_R-v_2}{v_1-v_R}\right)-\exp\left(k_0A\dfrac{v_R-v_2}{v_1-v_R}\right)\right), & \tau>D \end{cases}$$

$$C\le A<D\le B \tag{A8}$$

(6) If $C\le A<B\le D$ then c_1 and k are both non-zero only in the interval $A\le\tau\le B$ and so:

$$c_2=\begin{cases} 0, & \tau<A \\ c_{10}\dfrac{v_1-v_R}{v_R-v_2}\exp\left(k_0\dfrac{L-l_R-\xi}{v_1-v_R}\right)\left(\exp\left(k_0\tau\dfrac{v_R-v_2}{v_1-v_R}\right)-\exp\left(k_0A\dfrac{v_R-v_2}{v_1-v_R}\right)\right), & A\le\tau\le B \\ c_{10}\dfrac{v_1-v_R}{v_R-v_2}\exp\left(k_0\dfrac{L-l_R-\xi}{v_1-v_R}\right)\left(\exp\left(k_0B\dfrac{v_R-v_2}{v_1-v_R}\right)-\exp\left(k_0A\dfrac{v_R-v_2}{v_1-v_R}\right)\right), & \tau>B \end{cases}$$

$$C\le A<B\le D \tag{A9}$$

II. Let us now study the case: $v_R<v_2<v_1$. So now v_2-v_1 is negative and Eq. (16) will have the following form:

$$c_1(\xi,\tau)=\left\{\begin{matrix} c_{10}, & \dfrac{\xi-l_S}{v_1-v_2}\le\tau\le\dfrac{\xi}{v_1-v_2} \\ 0, & \tau<\dfrac{\xi-l_S}{v_1-v_2},\tau>\dfrac{\xi}{v_1-v_2} \end{matrix}\right\} \cdot \begin{cases} 1, \tau<\dfrac{L-l_R-\xi}{v_2-v_R} \\ \exp\left(k_0\dfrac{L-l_R-\xi+(v_R-v_2)\tau}{v_1-v_R}\right), \dfrac{L-l_R-\xi}{v_2-v_R}\le\tau\le\dfrac{L-\xi}{v_2-v_R} \\ \exp\left(-k_0\dfrac{l_R}{v_1-v_R}\right), \tau>\dfrac{L-\xi}{v_2-v_R} \end{cases} \tag{A10}$$

Let us define:

$$A=\frac{\xi-l_S}{v_1-v_2}, B=\frac{\xi}{v_1-v_2}, C=\frac{L-l_R-\xi}{v_2-v_R}, D=\frac{L-\xi}{v_2-v_R} \tag{A11}$$

Eq. (17) for k keeps the same form (Eq. (A3)). Now it is easy to see that equations for c_1 (Eq. (A10)) and for k in terms of A, B, C and D are the same as Eqs. (A2) and (A3) in the former case ($v_R<v_1<v_2$). Conditions $A<B$ and $C<D$ are right again, so Eqs.

(A4–A9) give the solution for the case $v_R < v_2 < v_1$ as well as for the former case ($v_k < v_1 < v_2$) with the only difference being that the new A and B are defined according to Eq. (A11).

III. Let us now study the case $v_2 < v_R < v_1$.

Eqs. (16) and (17) must now be written in the form:

$$c_1(\xi,\tau) = \begin{Bmatrix} c_{10}, & \frac{\xi - l_S}{v_1 - v_2} \le \tau \le \frac{\xi}{v_1 - v_2} \\ 0, & \tau < \frac{\xi - l_S}{v_1 - v_2}, \tau > \frac{\xi}{v_1 - v_2} \end{Bmatrix} \cdot \begin{Bmatrix} \exp\left(-k_0 \frac{l_R}{v_1 - v_R}\right), & \tau < \frac{\xi - L}{v_R - v_2} \\ \exp\left(k_0 \frac{L - l_R - \xi + (v_R - v_2)\tau}{v_1 - v_R}\right), & \frac{\xi - L}{v_R - v_2} \le \tau \le \frac{\xi - L - l_R}{v_R - v_2} \\ 1, & \tau > \frac{\xi - L + l_R}{v_R - v_2} \end{Bmatrix} \tag{A12}$$

$$k(\xi + (v_2 - v_R)\tau) = \begin{cases} k_0, & \frac{\xi - L}{v_R - v_2} \le \tau \le \frac{\xi - L + l_R}{v_R - v_2} \\ 0, & \tau < \frac{\xi - L}{v_R - v_2}, \tau > \frac{\xi - L + l_R}{v_R - v_2} \end{cases} \tag{A13}$$

Let us define:

$$A = \frac{\xi - l_S}{v_1 - v_2}, B = \frac{\xi}{v_1 - v_2}, C = \frac{\xi - L}{v_R - v_2}, D = \frac{\xi - L + l_R}{v_R - v_2}$$

Rewritten in the terms of A, B, C and D, Eq. (A12) has the following form:

$$c_1(\xi,\tau) = \begin{Bmatrix} c_{10}, & A \le \tau \le B \\ 0, & C < A, \tau > B \end{Bmatrix} \cdot \begin{Bmatrix} \exp\left(-k_0 \frac{l_R}{v_1 - v_R}\right), & \tau < C \\ \exp\left(k_0 \frac{L - l_R - \xi + (v_R - v_2)\tau}{v_1 - v_R}\right), & C \le \tau \le D \\ 1, & \tau > D \end{Bmatrix} \tag{A14}$$

while Eq. (A13) has the same form as Eq. (A3):

$$k(\xi + (v_2 - v_R)\tau) = \begin{cases} k_0, & C \le \tau \le D \\ 0, & \tau > C, \tau > D \end{cases} \tag{A15}$$

Comparing Eq. (A14) with Eq. (A2), one can see the difference between these equations is in values of c_1 for $\tau < C$ and $\tau > D$, but the values of c_1 in these intervals do not influence the result because, in these intervals, $k = 0$.

So Eqs. (A4–A9) are valid and give the analytical solution of Eqs. (15)–(17) for all three possible cases, but the values of A, B, C and D are different for these cases:

$$\text{if } v_R < v_1 < v_2 \quad \text{then } A = \frac{-\xi}{v_2 - v_1},$$

$$B = \frac{l_S - \xi}{v_2 - v_1}, C = \frac{L - l_R - \xi}{v_2 - v_R}, D = \frac{L - \xi}{v_2 - v_R}$$

$$\text{if } v_R < v_2 < v_1 \quad \text{then } A = \frac{\xi - l_S}{v_1 - v_2},$$

$$B = \frac{\xi}{v_1 - v_2}, C = \frac{L - l_R - \xi}{v_2 - v_R}, D = \frac{L - \xi}{v_2 - v_R}$$

$$\text{if } v_2 < v_R < v_1 \quad \text{then } A = \frac{\xi - l_S}{v_1 - v_2},$$

$$B = \frac{\xi}{v_1 - v_2}, C = \frac{\xi - L}{v_R - v_2}, D = \frac{\xi - L + l_R}{v_R - v_2} \tag{A16}$$

IV. Let us consider the special case: $v_2 = v_R < v_1$, then Eq. (15) has the form

$$\frac{\partial c_2}{\partial \tau} = k(\xi) \cdot c_1(\xi,\tau) \tag{A17}$$

where

$$c_1(\xi,\tau) = \begin{Bmatrix} c_{10}, & \frac{\xi - l_S}{v_1 - v_R} \le \tau \le \frac{\xi}{v_1 - v_R} \\ 0, & \tau < \frac{\xi - l_S}{v_1 - v_R}, \tau > \frac{\xi}{v_1 - v_R} \end{Bmatrix} \cdot \begin{Bmatrix} 1, & \xi < L - l_R \\ \exp\left(k_0 \frac{L - l_R - \xi}{v_1 - v_R}\right), & L - l_R < \xi < L \\ \exp\left(-k_0 \frac{l_R}{v_1 - v_R}\right), & \xi > L \end{Bmatrix}$$

$$k(\xi) = \begin{cases} k_0 & L - l_R < \xi < L \\ 0, & \xi < L - l_R, \xi > L \end{cases}$$

The solution of Eq. (A17) is:

$$c_2(\xi,\tau) = k(\xi) \cdot \int_0^\tau c_1(\xi,\tau)\, d\tau$$

and so,

$$c_2(\xi,\tau) = = \left\{ \begin{array}{cc} k_0 \exp\left(k_0 \dfrac{L - l_R - \xi}{v_1 - v_R}\right), & L - l_R \le \xi \le L \\ 0, & \xi < L - l_R,\ \xi > L \end{array} \right\} \cdot \left\{ \begin{array}{c} 0,\ \tau < \dfrac{\xi - l_S}{v_1 - v_R} \\ c_{10}\left(\tau - \dfrac{\xi - l_S}{v_1 - v_R}\right),\ \dfrac{\xi - l_S}{v_1 - v_R} \le \tau \le \dfrac{\xi}{v_1 - v_R} \\ c_{10}\dfrac{l_S}{v_1 - v_R},\ \tau > \dfrac{\xi}{v_1 - v_R} \end{array} \right. \quad \text{(A18)}$$

V. For another special case: $v_R < v_1 = v_2$, there is no need to change the variables second time and product concentration is determined by the equation:

$$\frac{\partial c_2}{\partial T} = k(\eta + (v_1 - v_R)T) \cdot c_1(\eta,T) \quad \text{(A19)}$$

where

$$c_1(\eta,T) = \left\{ \begin{array}{cc} c_{10}, & 0 < \eta < l_S \\ 0, & \eta < 0,\ \eta > l_S \end{array} \right\} \cdot \left\{ \begin{array}{c} 1,\ T < \dfrac{L - l_R - \eta}{v_1 - v_R} \\ \exp\left(-k_0\left(T - \dfrac{L - l_R - \eta}{v_1 - v_R}\right)\right),\ \dfrac{L - l_R - \eta}{v_1 - v_R} < T < \dfrac{L - \eta}{v_1 - v_R} \\ \exp\left(-k_0 \dfrac{l_R}{v_1 - v_R}\right),\ T > \dfrac{L - \eta}{v_1 - v_R} \end{array} \right.$$

So, the solution of Eq. (A19) is:

$$c_2(\eta,T) = \left\{ \begin{array}{cc} c_{10}, & 0 \le \eta \le l_S \\ 0, & \eta < 0,\ \eta > l_S \end{array} \right\} \cdot \left\{ \begin{array}{c} 1,\ T < \dfrac{L - l_R - \eta}{v_1 - v_R} \\ 1 - \exp\left(-k_0\left(T - \dfrac{L - l_R - \eta}{v_1 - v_R}\right)\right),\ \dfrac{L - l_R - \eta}{v_1 - v_R} \le T \le \dfrac{L - \eta}{v_1 - v_R} \\ 1 - \exp\left(-k_0 \dfrac{l_R}{v_1 - v_R}\right),\ T > \dfrac{L - \eta}{v_1 - v_R} \end{array} \right. \quad \text{(A20)}$$

Thus, Eqs. (A4–A9), A16, A18, A20) give the analytical solution to Eq. (15) for all possible values of v_1, v_R, v_2, l_S, l_R and L.

References

[1] V.P. Andreev, Russian Pat. Appl., 93 036 828, July 19 1993; positive decision November 29, 1995.
[2] V.P. Andreev, A.G. Kamenev, N.S. Popov, Talanta 43 (1996) 909.
[3] J. Bao, F.E. Regnier, J. Chromatogr. 608 (1992) 217.
[4] B.J. Harmon, D.H. Patterson, F.E. Regnier, Anal. Chem. 65 (1993) 2655.
[5] D.H. Patterson, B.J. Harmon, F.E. Regnier, J. Chromatogr. A 732 (1996) 119.
[6] L. Valtcheva, J. Mohammad, G. Patterson, S. Hjerten, J. Chromatogr. 638 (1993) 263.
[7] I. Haumann, K. Bachmann, J. Chromatogr. A 717 (1995) 385.
[8] V.P. Andreev, E.E. Lisin, Chromatographia 37 (1993) 202.
[9] F. Regan, M. Meaney, S. Lunte, J. Chromatogr. B 657 (1994) 409.